JOURNAL OF SOLID STATE CHEMISTRY 36, 20–27 (1981)

About Stannous Fluoride SnF_2. III. Thermal Expansion

G. DÉNÈS*

Laboratoire de Chimie Minérale D, Laboratoire associé au CNRS No. 254, Université de Rennes I, 35042 Rennes Cédex, France

Received December 5, 1979; in revised form March 7, 1980

The unit-cell parameters of SnF_2 were measured from −200 to 190°C. The tensor of thermal expansion of the three phases (α, β, and γ) was computed from the expansion in each (*hkl*) direction by a least-squares method. The thermal expansion of each phase is related to its crystal structure and physical properties (molecular structure of α-SnF_2, ferroelastic properties of the β-phase).

Introduction

The study of the thermal expansion of crystalline solids gives much useful information on the strength of bonds in crystals and the thermal stability of crystalline networks. Many studies have been devoted to the thermal expansion of ionic compounds (e.g., fluorite and rutile types) and molecular organic compounds (especially cyclic compounds). However, little is known about inorganic materials with molecular features. The characteristics of SnF_2, intermediate between ionic and molecular (isolated Sn_4F_8 tetramers in α-SnF_2, three-dimensional lattice of β- and γ-SnF_2), make it a suitable material for the investigation of its dilatation. Furthermore, two phase transitions ($\alpha \rightarrow \gamma$ and $\beta \rightleftharpoons \gamma$) were detected in the study of the unit-cell parameters versus temperature. The knowledge of the thermal expansion at the phase transitions gives useful information on the mechanism of these transitions.

* Present address: McMaster University, Department of Chemistry, 1280 Main Street West, Hamilton, Ontario L8S 4M1, Canada.

0022-4596/81/010020-08$02.00/0

1. Experimental

1.1. Data Collection

The starting material, monoclinic α-SnF_2, was supplied by OSI. High-temperature X-ray data were collected with a Gerard–Barret furnace (*1*) attached to a CGR powder diffractometer. Samples were 2.5-cm-diameter pellets prepared under 1000 kg/cm². All experiments were carried out under dry nitrogen. For low-temperature measurements, we used a liquid nitrogen attachment devised in this laboratory (*2*) and mounted on the same diffractometer. No internal standard was used since most react with SnF_2 at high temperature. The furnace was first calibrated with several standards.

In order to prevent the oxidation and/or hydrolysis of the samples, we did not record the whole powder pattern at each temperature but used the following procedure: the temperature of the sample was slowly increased and a few reflections were recorded as the temperature change was less than 2°C during the time required to record each peak. After each thermal cycle

(a few hours) the sample was changed to study some other reflections. The powder pattern of α-SnF_2 was studied from -200 to 150°C (temperature of the $\alpha \rightarrow \gamma$ transition), β-SnF_2 from -200 to 66°C (temperature of the $\beta \rightleftharpoons \gamma$ transition), and γ-SnF_2 from 66 to 190°C, in steps of 20°C.

1.2. *Mathematical Treatment*

At each temperature, the unit-cell parameters were least-squares refined (*3*) from the interplanar spacing d_{hkl}. The expansion α_{hkl} in each $[hkl]^*$ direction normal to the (hkl) plane was obtained from the evolution of each d_{hkl} with temperature.

$$\alpha_{hkl} = \frac{1}{d_{hkl}} \cdot \frac{\partial d_{hkl}}{\partial T}. \qquad \text{(I)}$$

Each α_{hkl} coefficient can be expressed as a linear function of the six thermal expansion coefficients α_{ij}:

$$\alpha_{hkl} = \alpha_{11}b_1 + \alpha_{22}b_2 + \alpha_{33}b_3 + \alpha_{32}b_4 + \alpha_{31}b_5 + \alpha_{21}b_6. \qquad \text{(II)}$$

The coefficients b_i to b_6 are functions of the unit-cell parameters and the (hkl) indices. The tensor of thermal expansion α_{ij} is obtained from the α_{hkl} values by a least-squares method (*4*). The principal coefficients α_i and the orientation of the principal directions of thermal expansion are obtained in the monoclinic case by Mohr's method (*5*), using the following relations:

$$\alpha_1 = \frac{\alpha_{11} + \alpha_{33}}{2} - r, \qquad \text{(III)}$$

$$\alpha_3 = \frac{\alpha_{11} + \alpha_{33}}{2} + r, \qquad \text{(IV)}$$

$$tg\ 2\psi = \frac{2\,|\alpha_{31}|}{\alpha_{11} - \alpha_{33}}, \qquad \text{(V)}$$

with

$$r^2 = \frac{(\alpha_{33} - \alpha_{11})^2}{4} + \alpha_{31}^2. \qquad \text{(VI)}$$

In monoclinic symmetry, the α_2 direction is oriented along the **b** axis ($\alpha_2 = \alpha_{22}$), whereas α_1 and α_3 lie in the (**a**, **c**) plane (Neuman principle (*5*)). Their orientation in this plane, not imposed by the symmetry, is given by the ψ angle between the **a** axis and the direction of α_1.

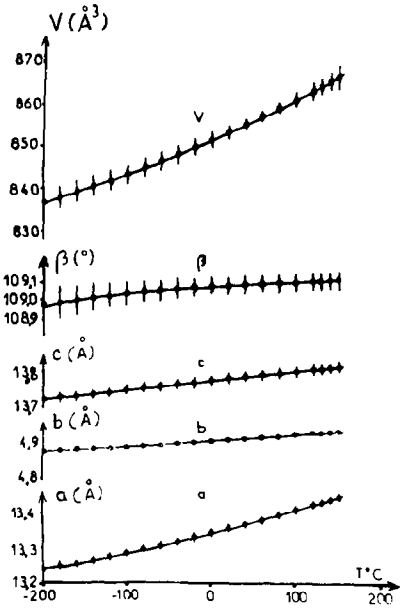

FIG. 1. Unit-cell parameters of α-SnF_2 versus temperature.

2. Results

The evolution of the unit-cell parameters of α-SnF_2 versus temperature is given in Fig. 1. The cell parameters can be evaluated as a function of temperature T(°K) from the polynomial

$$a(T) = a_0 + a_1 \times T + a_2 \times T^2 \qquad \text{(VII)}$$

(a = unit-cell parameters a, b, c in Å, V in Å^3, and β in (°)). The numerical values of the coefficients a_0, a_1, and a_2 are given in Table I. For β-SnF_2 the values of a and b cannot be evaluated by a single polynomial because of the large expansion in the vicinity of the $\beta \rightleftharpoons \gamma$ transition; they were fitted to two polynomials, one below -40°C, the

TABLE I

FITTED POLYNOMIALS FOR THE EVOLUTION OF THE UNIT-CELL PARAMETERS VERSUS TEMPERATURE T (°K)

Phase	T(°K)	Parameter	a_0 (Å)	a_1 (Å K^{-1})	a_2 (Å K^{-2})
α	$73 < T < 423$	a(Å)	13.216	2.81×10^{-4}	6.2×10^{-7}
		b(Å)	4.864	1.00×10^{-4}	1.4×10^{-7}
		c(Å)	13.694	3.34×10^{-4}	-1.1×10^{-7}
		β(°)	108.92	8.6×10^{-4}	$-9. \times 10^{-7}$
		V(Å^3)	832.75	5.0×10^{-2}	$6. \times 10^{-5}$
β	$73 < T < 233$	a(Å)	4.836	-6.95×10^{-5}	1.9×10^{-6}
		b(Å)	5.211	6.17×10^{-5}	-8.4×10^{-7}
	$233 < T < 339$	a(Å)	5.202	-2.95×10^{-3}	7.6×10^{-6}
		b(Å)	4.835	3.20×10^{-3}	-7.4×10^{-6}
	$73 < T < 339$	c(Å)	8.418	1.96×10^{-4}	5.8×10^{-8}
		V(Å^3)	211.41	1.5×10^{-2}	$2. \times 10^{-5}$
γ	$339 < T < 463$	a(Å)	5.090	-2.85×10^{-4}	6.6×10^{-7}
		c(Å)	8.755	-1.53×10^{-3}	2.2×10^{-6}
		V(Å^3)	226.55	-6.3×10^{-2}	$1. \times 10^{-4}$

other between −40 and 66°C. Such a behavior is common when an order parameter is associated with a phase transition (*6*).

In a similar way, the principal coefficients of thermal expansion can be evaluated as a linear function of temperature T (°K) (Figs. 2 and 3),

$$\alpha_i(T) = \alpha' + \alpha'' \times T, \qquad \text{(VIII)}$$

except α_3 of α- and β-SnF_2 which is constant within the experimental precision ($\sigma_{\alpha_3} = 0.28 \times 10^{-6}$). The coefficients α_i are given in °K^{-1} (Table II).

To our knowledge, only the study of Acker *et al.* (*7*) was previously devoted to

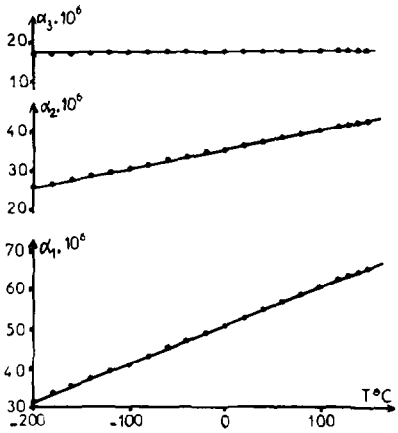

FIG. 2. Principal coefficients of thermal expansion of α-SnF_2 versus temperature.

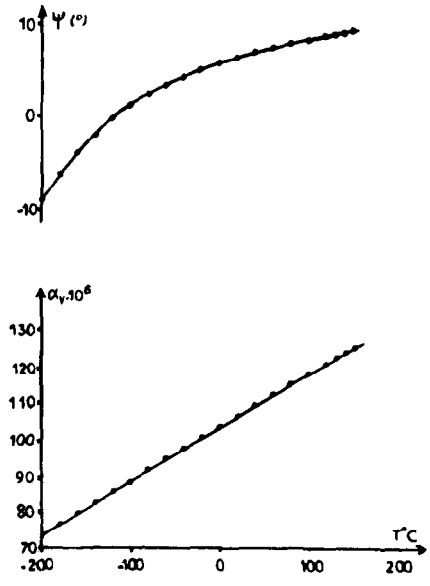

FIG. 3. Volume expansion and ψ angle (orientation of the thermal expansion tensor in the (a, c) plane) of α-SnF_2 versus temperature.

TABLE II

FITTED POLYNOMIALS FOR THE EVOLUTION OF THE TENSOR OF THERMAL EXPANSION VERSUS TEMPERATURE T (°K)

Phase	T(°K)	α_i	α'	α''
α-SnF_2	$73 < T < 423$	α_1	24.2×10^{-6}	9.6×10^{-8}
		α_2	21.9×10^{-6}	4.8×10^{-8}
		α_3	17.4×10^{-6}	0
		α_V	63.0×10^{-6}	14.7×10^{-8}
β-SnF_2	$73 < T < 233$	α_1	-26.7×10^{-6}	8.5×10^{-7}
		α_2	10.8×10^{-6}	-3.3×10^{-7}
		α_V	9.5×10^{-6}	5.1×10^{-7}
	$233 < T < 339$	α_1	-629.6×10^{-6}	3.2×10^{-6}
		α_2	643.0×10^{-6}	-3.0×10^{-6}
		α_V	86.9×10^{-6}	8.2×10^{-8}
	$73 < T < 339$	α_3	24.6×10^{-6}	0
γ-SnF_2	$339 < T < 463$	α_1	-65.3×10^{-6}	3.3×10^{-7}
		α_3	-225.4×10^{-6}	6.4×10^{-7}
		α_V	-356.1×10^{-6}	1.2×10^{-6}

the thermal expansion of tin difluoride. These authors measured the thermal expansion coefficients of α-SnF_2 between 0 and 20°C; they used a different experimental method (using a Fizeau interferometer). Good agreement is observed between their results and ours at 10°C (the standard deviations are given in parentheses):

	Acker *et al.* (*7*)	This work
$\alpha_{11} \times 10^6$	58.4(1.8)	51.3(6)
$\alpha_{22} \times 10^6$	37.7(1.2)	35.7(6)
$\alpha_{33} \times 10^6$	16.7(5)	18.0(6)
$\alpha_{31} \times 10^6$	5.5(6)	3.5(4)

3. Discussion

3.1. Volume Expansion

We previously showed the structural relationships between SnF_2 and ionic fluorides (cationic lattice as in the rutile type, Sn_6F_6 rings as in the cristobalite) (*8*). Their volume expansions are compared in Tables III and IV.

Megaw (*9*) has explained that the mean linear expansion coefficient $\bar{\alpha}_l$ is inversely proportional to the square of the electrostatic valence q for three-dimensional structures (fluorite and rutile types). We can see (Table III) that SnF_2 and PbF_2 do not conform to this rule. The very high volume expansion can be attributed to the lone pair–fluorine atom repulsions for PbF_2 and SnF_2, and to the molecular characteristics for α-SnF_2 (presence of Sn_4F_8 tetra-

TABLE III

COMPARISON OF THE EXPERIMENTAL VOLUME EXPANSION WITH THE VALUE CALCULATED FROM THE ELECTROSTATIC VALENCE q (*9*)

Compound	T(°C)	$3 \times (1/q^2)$	$\alpha_V \times 10^6$	Reference
α-SnF_2	20	12	101.6	This work
β-SnF_2	20	19	107.6	This work
MgF_2	20	27	30.9	(*11*)
SnO_2	20	7	11.4	(*11*)
CaF_2	20	48	57.3	(*11*)
SrF_2	20	48	55.7	(*11*)
BaF_2	20	48	59.4	(*11*)
α-PbF_2	20	61	109.4	(*12*)
β-PbF_2	35	48	86.4	(*13*)

TABLE IV

COMPARISON OF THE THERMAL EXPANSION OF γ-SnF_2 WITH THAT OF α- AND β-CRISTOBALITE

Compound	T(°C)	$\alpha_1 \times 10^6$	$\alpha_3 \times 10^6$	$\alpha_v \times 10^6$	Reference
γ-SnF_2	70	32.8	−5.4	60.2	This work
γ-SnF_2	190	67.2	71.6	206.0	This work
α-Cristobalite	70	19.5	52.5	91.5	(*14*)
α-Cristobalite	190	19.5	52.2	91.2	(*14*)
β-Cristobalite	350	7.8	7.8	23.4	(*15*)

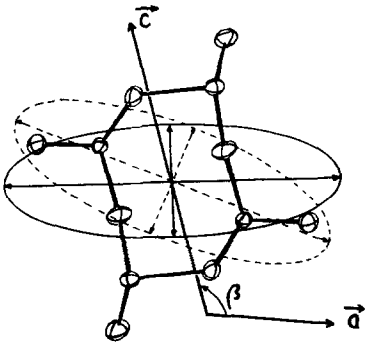

FIG. 4. α-SnF_2: projection of a Sn_4F_8 tetramer and of the ellipsoid of thermal expansion (full line) and hydrostatic compressibility (dashed line) in the (a, c) plane.

mers) (*10*). The presence of the nonbonding electron pairs of tin atoms inside the Sn_6F_6 rings of γ-SnF_2 gives strong lone pair–fluorine repulsions from which a large expansion results; in the α- and β-cristobalite, the Si_6O_6 rings are empty and therefore the expansion is weaker.

3.2. Anisotropy of Expansion and Compressibility of α-SnF_2

3.2.1. Thermal expansion anisotropy. Many studies devoted to cyclic molecular compounds (e.g., hexamethylbenzene (*16*), nitroaniline, and *p*-dinitrobenzene (*17*)) have emphasized the strong anisotropy of their thermal expansion. On the contrary, the thermal expansion of ionic compounds exhibiting three-dimensional structures is barely anisotropic. This is illustrated in Table V: the anisotropy of thermal expansion for α-SnF_2 appears as being intermediate between ionic and molecular compounds. The main feature of molecular compounds is the very large expansion perpendicular to the plane of a large flat molecule, i.e., in the direction where only van der Waals interactions occur. On the other hand, in ionic compounds, the largest expansion lies in the direction of the strongest interionic repulsions, in agreement with Pauling's third rule (*19*). For α-SnF_2, the expansion normal to the mean plane of the Sn_4F_8 tetramers ($\alpha_2 = 36.1 \times 10^{-6}$ at 20°C) is not the largest one; this result is in agreement with its crystal structure (*10, 20*) being intermediate between that of ionic (analogous to the rutile type, anionic packing) and molecular compounds (presence of Sn_4F_8 tetramers, Sn–F distances which are 10% shorter than the sum of the ionic radii of Sn^{2+} and F^-, suggesting that the bonding is predominantly covalent). It follows that the Sn–F interactions between neighboring tetramers are stronger than the van der Waals interactions observed in organic crystals.

The orientation of the ellipsoid in the (a, c) plane and the values of α_1 and α_3 coefficients depend only on the interatomic repulsions (*21*); the results are in good agreement with the crystal structure. The rule proposed by Megaw (*9*) for molecular compounds works well: it assumes that in a given direction, the coefficient of thermal expansion is the sum of two components, one within the molecule and the other intermolecular. The intramolecular components of α_1 and α_3 are explained in Fig. 4: the thermal expansion coefficient is a maximum in the direction of the smallest size of the molecule and a minimum in the direction of its largest dimension. The intermolecular components (Fig. 5) result from the repulsions between the fluorine atoms of each tetramer (each tetramer being considered rigid) and the lone pairs of the tin atoms of its neighboring tetramers.

TABLE V

ANISOTROPY OF THE THERMAL EXPANSION IN α-SnF_2, COMPARED TO THE BEHAVIOR OF IONIC (MgF_2) AND MOLECULAR (HEXAMETHYLBENZENE) COMPOUNDS

Compound	T(°C)	$\alpha_1 \times 10^6$	$\alpha_2 \times 10^6$	$\alpha_3 \times 10^6$	Reference
α-SnF_2	20	52.4	36.1	17.6	This work
MgF_2	25	9.4	9.4	13.6	(*18*)
Hexachloromethylbenzene	−25	209	48	30	(*16*)

3.2.2. Hydrostatic compressibility. The elastic stiffness C_{ij} and elastic moduli coefficients S_{ij} of α-SnF_2 were previously determined by Acker *et al.* (*7, 22*) at room temperature. From these results one can calculate the compressibility tensor β_{ij} using the relations given by Nye (*5*); the principal coefficients of compressibility at room temperature are as follows (β are given in bar^{-1}):

$$\beta_1 = 1.931 \times 10^{-6} \qquad \beta_2 = 3.417 \times 10^{-6}$$
$$\beta_3 = 0.717 \times 10^{-6} \qquad \psi = 16.7°$$

The largest compressibility (β_2) is along the **b** axis since the interactions between the tetramers are a minimum in this direction. The projection of the ellipsoid of compressibility on the (**a**, **c**) plane is given in Figs. 4 and 5. As for the thermal expansion, we can assume that the compressibility coefficients β_1 and β_3 are the sum of an intramolecular and an intermolecular component. Within a molecule, the largest compressibility (β_1) occurs in the direction of the shortest Sn–Sn distance (Fig. 4), and the smallest compressibility (β_3) in the direction of the largest Sn–Sn distance; consequently, the intramolecular component is negligible. The largest compressibility lies in almost the same direction as the farthest tetramers and the smallest compressibility lies in almost the same direction as the nearest tetramers as shown in Fig. 5. Therefore, the only effect of hydrostatic pressure is to bring the tetramers closer to each other without distorting them. This behavior is characteristic of molecular solids.

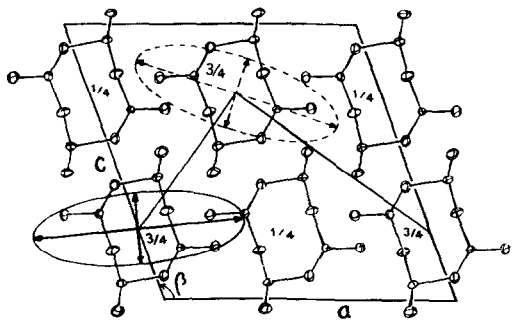

FIG. 5. α-SnF_2: Projection of the Sn_4F_8 tetramers and of the ellipsoid of thermal expansion (full line) and hydrostatic compressibility (dashed line) in the (**a**, **c**) plane.

3.3. Ferroelasticity of β-SnF_2

The thermal expansion of β-SnF_2 is strongly anisotropic, especially in the (**a**, **b**) plane (large expansion along **a**, large contraction along **b**) (Figs. 6 and 7). The most notable feature of the $\gamma \rightarrow \beta$ transition is the splitting of the *hkl* and *hk*0 lines corresponding to the orthorhombic distortion. These splittings disappear at 66°C; the corresponding transition is pure ferroparaelastic phase transition of the 422F222 type in Aizu's notation (*23, 24*). As no discontinuity of the unit-cell parameters or volume, and no heat of transition, is observed, but only a change of specific heat and thermal expansion coefficients, this transition is a second-order displacive one. Furthermore, the symmetry of the crystal allows the transition to be continuous ($P4_12_12$ or $P4_32_12 \rightarrow P2_12_12_1$) The most obvious feature of the transition from the prototype

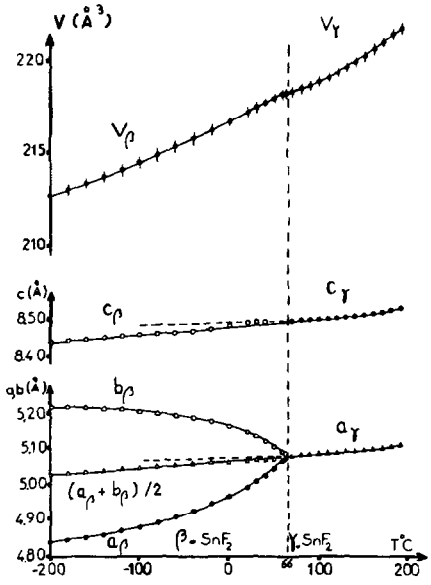

FIG. 6. Evolution of the unit-cell parameters of β- and γ-SnF_2 with temperature.

phase (γ) to the ferroelastic phase (β) is the splitting of the tetragonal a parameter into two different a and b parameters. Furthermore a discontinuity of the first derivatives of c, $(a + b)$, and the volume occur as in the similar transition for TeO_2 under pressure (*25, 26*). The result is that the orthorhombic parameters a_0, b_0, c_0 can be expressed as a function of the tetragonal parameters a_T and c_T as

$$\begin{vmatrix} a_0 \\ b_0 \\ c_0 \end{vmatrix} = \begin{vmatrix} 1 + e_1 & 0 & 0 \\ 0 & 1 + e_2 & 0 \\ 0 & 0 & 1 + e_3 \end{vmatrix} \begin{vmatrix} a_T \\ a_T \\ c_T \end{vmatrix},$$

where e_1, e_2, e_3 are the distortions respectively along **a**, **b**, and **c**. The transition is characterized by three order parameters $\eta_1 = e_2 - e_1$, $\eta_2 = e_1 + e_2$, $\eta_3 = e_3$. η_1 is a primary order parameter (it is responsible for the breaking of symmetry at the transition) while η_2 and η_3 are secondary (they respect the tetragonal symmetry).

3.4. Aspherism Index. Stability of the α- and β-Phases

In studying the variation of the symmetry of the thermal expansion tensor as a function of temperature, Weigel *et al.* (*27, 28*) have defined a measure of this symmetry called the "aspherism index." They observed that this aspherism index decreases when the temperature increases except in the phases which present a phase transition at higher temperature. As shown in Fig. 8, the aspherism index of α-SnF_2 increases with temperature in agreement with Weigel's observations on ordered phases. Consequently, a phase transition at high temperature can be expected; indeed it

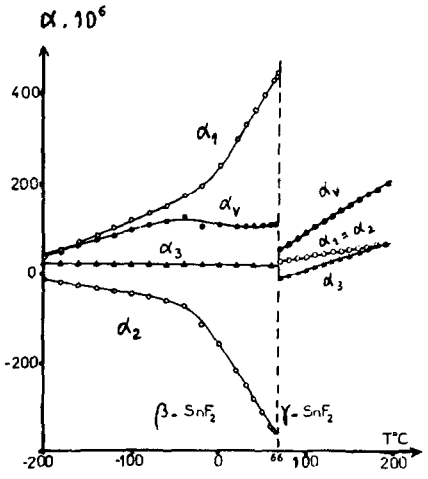

FIG. 7. Evolution of the thermal expansion tensor of β- and γ-SnF_2 with temperature.

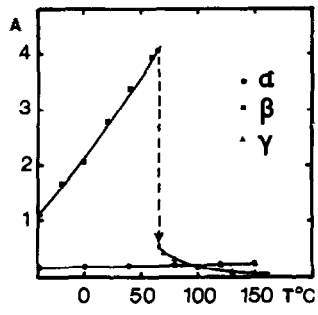

FIG. 8. Aspherism index A of SnF_2 as a function of temperature.

undergoes a first-order phase transition ($\alpha \rightarrow \gamma$) around 150°C (*4*).

The increase with temperature in the β-phase indicates that this phase gets less and less stable at high temperature. A very sharp increase as in the vicinity of the $\beta \rightleftharpoons \gamma$ transition is commonly encountered for phase transitions associated with an order parameter: in this case, the measured thermal expansion is the sum of the "true thermal expansion" (caused by the anharmonicity of the thermal vibrations) and the distortion of the cell associated with the transition, which is most of the time much higher than the true thermal expansion (*28*). At the $\beta \rightarrow \gamma$ phase transition, the aspherism index drops (from 4.10 to 0.45); its behavior in the γ-phase is "normal": it decreases when temperature increases so that the expansion is isotropic ($\alpha_1 = \alpha_3$ is not imposed by the tetragonal symmetry) just before the melting point. A similar behavior is observed in the cristobalite (similar crystal structure): the expansion is anisotropic in the α-phase until the $\alpha \rightarrow \beta$ transition, and isotropic in the β-phase.

References

1. P. Barret, N. Gerard, and G. Watelle-Marion, *Bull. Soc. Chim. Fr.* **8,** 3172 (1972).
2. P. Charbit and P. Ducros, *Bull. Soc. Fr. Miner. Cristallogr.* **91,** 116 (1968).
3. J. Y. Le Marouille, Thèse de 3ème cycle, Université de Rennes, Rennes (1972).
4. G. Dénès, Thèse d'Etat, Université de Rennes, Rennes (1978).
5. J. F. Nye, "Physical Properties of Crystals," Oxford Univ. Press (Clarendon), London (1957).
6. P. Garnier, G. Calvarin, and D. Weigel, *J. Solid State Chem.* **16,** 55 (1976).
7. E. Acker, K. Recker, S. Haussühl, and H. Siegert, *Z. Naturforsch. A* **26,** 1766 (1971).
8. G. Dénès, J. Pannetier, and J. Lucas, *J. Solid State Chem.* **33,** 1 (1980).
9. H. D. Megaw, "Crystal Structures: A Working Approach," Saunders, Philadelphia (1973).
10. G. Dénès, J. Pannetier, J. Lucas, and J. Y. Le Marouille, *J. Solid State Chem.* **30,** 335 (1979).
11. Y. S. Touloukian, R. K. Kirby, R. E. Taylor, and T. Y. R. Lee, "Thermophysical Properties of Matter," Vol. 13, IFI/Plenum, New York (1977).
12. V. K. Mahajan, P. T. Chang, and J. L. Margrave, *High Temp.–High Pressures* **7,** 325 (1975).
13. P. Pascal, "Nouveau Traité de chimie minérale," Vol. 9, p. 351, Masson, Paris (1958).
14. D. R. Peacor, *Z. Kristallogr. Kristallogeometrie Kristallophys. Kristallochem.* **138,** 274 (1973).
15. A. F. Wright and A. J. Leadbetter, *Phil. Mag.* **31,** 1391 (1975).
16. I. Woodward, *Acta Crystallogr.* **11,** 441 (1958).
17. P. J. A. McKeown, A. R. Ubelohde, and I. Woodward, *Acta Crystallogr.* **4,** 391 (1951).
18. K. V. K. Rao, *in* "Physics of the Solid State" (S. Balakrishna, Ed.), p. 415, Academic Press, New York (1969).
19. L. Pauling, *J. Amer. Chem., Soc.* **51,** 1010 (1929).
20. R. C. McDonald, H. Ho-Kuen Hau, and K. Eriks, *Inorg. Chem.* **15,** 4, 762 (1976).
21. J. Bouvais and D. Weigel, *Acta Crystallogr. Sect. A* **26,** 510 (1970).
22. E. Acker, S. Haussühl, and K. Recker, *J. Cryst. Growth* **13,** 74, 467 (1972).
23. K. Aizu, *J. Phys. Soc. Japan* **27,** 2, 387 (1969).
24. K. Aizu, *Phys. Rev. B* **2,** 3, 754 (1970).
25. E. F. Skelton, J. L. Feldman, C. Y. Liu, and J. L. Spain, *Phys. Rev. B* **13,** 6, 2605 (1976).
26. T. G. Worlton and R. A. Beyerlein, *Phys. Rev. B* **12,** 5, 1899 (1975).
27. D. Weigel, P. Garnier, and J. F. Berar, *C.R. Acad. Sci. Ser. C* **283,** 305 (1976).
28. D. Weigel, T. Beguemsi, P. Garnier, and J. F. Berar, *J. Solid State Chem.* **16,** 55 (1976).